AD-A116 900 HOWARD UNIV WASHINGTON DC DEPT OF CHEMISTRY F/G 7/4
RAMAN AND X-RAY INVESTIGATIONS OF ICE VII TO 36.0 GPA.(U)
JUN 82 G E WALRAFEN, M ABEBE, F A MAUER N00014-80-C-0305
UNCLASSIFIED TR-10 NL

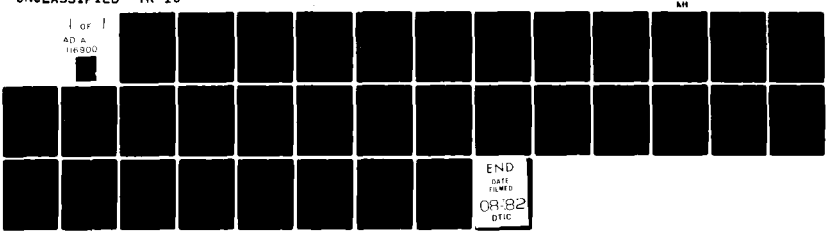

SECURITY CLASSIFICATION OF THIS PAGE (When Data Entered)

REPORT DOCUMENTATION PAGE		READ INSTRUCTIONS BEFORE COMPLETING FORM
1. REPORT NUMBER 10	2. GOVT ACCESSION NO. AD-A116900	3. RECIPIENT'S CATALOG NUMBER
4. TITLE (and Subtitle) Raman and X-Ray Investigations of Ice VII to 36.0 GPa		5. TYPE OF REPORT & PERIOD COVERED Technical Report #10 6. PERFORMING ORG. REPORT NUMBER
7. AUTHOR(s) G.E. Walrafen F.A. Mauer, S. Block M. Abebe G.J. Piermarini, R. Munro		8. CONTRACT OR GRANT NUMBER(s) N00014-80-C-0305
9. PERFORMING ORGANIZATION NAME AND ADDRESS Department of Chemistry Howard University Washington, D.C. 20059		10. PROGRAM ELEMENT, PROJECT, TASK AREA & WORK UNIT NUMBERS NR-051-733
11. CONTROLLING OFFICE NAME AND ADDRESS Office of Naval Research Department of the Navy Arlington, Virginia, 22217		12. REPORT DATE June 30, 1982 13. NUMBER OF PAGES 29
14. MONITORING AGENCY NAME & ADDRESS(if different from Controlling Office)		15. SECURITY CLASS. (of this report) Unclassified 15a. DECLASSIFICATION/DOWNGRADING SCHEDULE

16. DISTRIBUTION STATEMENT (of this Report)

Approved for public release; reproduction is permitted for any purpose of the United States government distribution is unlimited.

17. DISTRIBUTION STATEMENT (of the abstract entered in Block 20, if different from Report)

Distribution of this document is unlimited

18. SUPPLEMENTARY NOTES

Prepared and accepted for publication in the Journal of Chemical Physics.

19. KEY WORDS (Continue on reverse side if necessary and identify by block number)

Raman Scattering, X-Ray, Ice VII, High Pressure

20. ABSTRACT (Continue on reverse side if necessary and identify by block number)

Raman data for ice VII to 30 GPa and x-ray lattice parameters to 36 GPa, all at room temperature, are presented and discussed. Both the Raman OH-stretching peak frequency ($\Delta\bar{\nu}$) and the edge distance of the body-centered cubic unit cell (a) decrease at a decreasing rate with pressure rise. The OH peak frequency is found to be virtually linear in the nearest-neighbor O-O distance (r_{OO}) between about 2.5 and 2.9 Å. However, the data can also be fitted with a slight cubic dependence, which when extrapolated, gives rise to a minimum in $\Delta\bar{\nu}$ at r_{OO} = 2.35 ± 0.06Å. This is close to the value of 2.4Å found for the sym-

DD FORM 1 JAN 73 1473 EDITION OF 1 NOV 65 IS OBSOLETE S/N 0102-014-6601

SECURITY CLASSIFICATION OF THIS PAGE (When Data Entered)

ABSTRACT CONTINUED

SECURITY CLASSIFICATION OF THIS PAGE *(When Data Entered)*

REPORT DOCUMENTATION PAGE		READ INSTRUCTIONS BEFORE COMPLETING FORM
1. REPORT NUMBER	2. GOVT ACCESSION NO.	3. RECIPIENT'S CATALOG NUMBER
4. TITLE *(and Subtitle)*		5. TYPE OF REPORT & PERIOD COVERED
		6. PERFORMING ORG. REPORT NUMBER
7. AUTHOR(s)		8. CONTRACT OR GRANT NUMBER(s)
9. PERFORMING ORGANIZATION NAME AND ADDRESS		10. PROGRAM ELEMENT, PROJECT, TASK AREA & WORK UNIT NUMBERS
11. CONTROLLING OFFICE NAME AND ADDRESS		12. REPORT DATE
		13. NUMBER OF PAGES
14. MONITORING AGENCY NAME & ADDRESS*(if different from Controlling Office)*		15. SECURITY CLASS. *(of this report)*
		15a. DECLASSIFICATION/DOWNGRADING SCHEDULE
16. DISTRIBUTION STATEMENT *(of this Report)*		
17. DISTRIBUTION STATEMENT *(of the abstract entered in Block 20, if different from Report)*		
18. SUPPLEMENTARY NOTES		
19. KEY WORDS *(Continue on reverse side if necessary and identify by block number)*		

20. ABSTRACT *(Continue on reverse side if necessary and identify by block number)*

metric O-H-O units in other materials. This minimum suggests, but does not prove, that a symmetric hydrogen bond structure, O-H-O, and thus a new ice, may result at pressures of about 75±20 GPa. Treatment of the O-H-O units according to coupled oscillators using experimentally confirmed assuptions indicates that $\Delta\bar{\nu} \approx A/r^2_{OH}$, which when combined with present and previously published data yields, approximately, $A \approx 2943$ cm^{-1}Å^2. Thus the decrease observed in is thought to occur because the OH bond length (r_{OH}) increases with increasing pressure as the O-O distance r_{OO} in the corresponding hydrogen-bonded O-H...O unit decreases.

DD FORM 1 JAN 73 1473 EDITION OF 1 NOV 65 IS OBSOLETE
S/N 0102-014-6601 |

SECURITY CLASSIFICATION OF THIS PAGE *(When Data Entered)*

RAMAN AND X-RAY INVESTIGATIONS OF ICE VII TO 36.0 GPa

G. E. Walrafen and M. Abebe
Chemistry Department
Howard University
Washington, DC 20059

and

F. A. Mauer, S. Block, G. J. Piermarini, and R. Munro
Center for Materials Science
National Bureau of Standards
Washington, DC 20234

ABSTRACT

Raman data for ice VII to 30 GPa and x-ray lattice parameters to 36 GPa, all at room temperature, are presented and discussed. Both the Raman OH-stretching peak frequency ($\Delta\tilde{\nu}$) and the edge distance of the body-centered cubic unit cell (a) decrease at a decreasing rate with pressure rise. The OH peak frequency is found to be virtually linear in the nearest-neighbor O-O distance (r_{OO}) between about 2.5 and 2.9 Å. However, the data can also be fitted with a slight cubic dependence, which when extrapolated, gives rise to a minimum in $\Delta\tilde{\nu}$ at $r_{OO} = 2.35 \pm 0.06$ Å. This is close to the value of 2.4 Å found for the symmetric O-H-O units in other materials. This minimum suggests, but does not prove, that a symmetric hydrogen bond structure, O-H-O, and thus a new ice, may result at pressures of about 75±20 GPa. Treatment of the O-H···O units according to coupled oscillators using experimentally confirmed assumptions indicates that $\Delta\tilde{\nu} \approx A/r_{OH}^2$, which when combined with present and previously published data yields, approximately, $A \approx 2943$ cm^{-1}Å^2. Thus the decrease observed in $\Delta\tilde{\nu}$ is thought to occur because the OH bond length (r_{OH}) increases with increasing pressure as the O-O distance r_{OO} in the corresponding hydrogen-bonded O-H···O unit decreases.

RAMAN AND X-RAY INVESTIGATIONS OF ICE VII TO 36.0 GPa

G. E. Walrafen and M. Abebe
Chemistry Department
Howard University
Washington, DC 20059

and

F. A. Mauer, S. Block, G. J. Piermarini, and R. Munro
Center for Materials Science
National Bureau of Standards
Washington, DC 20234

I. INTRODUCTION

Ice VII, discovered by Bridgman[1], is produced when ice VI is subjected to a pressure $\geq$ 2.14 GPa at room temperature[2]. X-ray diffraction data at high pressure indicate that ice VII has a body-centered cubic arrangement of oxygen atoms, with some degree of disorder of the protons[3,4,5]. In contrast, ice VIII, which forms when ice VII is cooled below -3 °C, is proton-ordered[6], and its oxygen arrangement, although originally thought to be the same as that of ice VII, probably involves slight tetragonal distortion, space group $I4_1/amd$[7,8].

An interesting feature common to ices VI, VII, and VIII, involves interpenetration of lattices. In the case of ice VII two interpenetrated, but unconnected, diamond-type (like ice I_c) lattices exist. Thus, the density of ice VII approaches twice that of ice I_h, and would be twice if it were not for an increase in the O-O distance r_{OO} above the ice I_h value of 2.76 Å. A further feature of ice VII that is related to the unconnected lattices, is that only four of the eight nearest-neighbor oxygen atoms are hydrogen-bonded to the central oxygen atom. The oxygen atoms of the two unconnected lattices engage in repulsive contacts which increase r_{OO} above 2.76 Å.

Of all of the phases of water known to exist thus far, the fluid phase (including the liquid and the dense supercritical fluid), and ice VII, have the greatest pressure range of stability[8]. Ice VII has been visually observed with a polarizing microscope to 50 GPa at room temperature with no obvious transition[9] and recently confirmed to 36 GPa by x-ray powder diffraction measurements[10]. No ice having symmetric hydrogen bonds has yet been produced. Such an ice would require very high pressures for its formation, calculated to be between 35 and 80 GPa[11].

The extreme pressure stability of ice VII is a feature which made the present Raman and x-ray study attractive. This large pressure range allowed for large variations in $\Delta\bar{\nu}$ and in the x-ray lattice parameter, a, compared, for example, to ice VI, where a similar study was impracticable[12]. Between 2.30 GPa and 36 GPa the body-centered cubic unit cell edge, a, decreased from 3.367 to 2.896 Å, and to 30 GPa, the Raman OH peak frequency, $\Delta\bar{\nu}$, decreased from about 3300 to 2800 cm^{-1}. These large decreases allowed the pressure dependences to be determined accurately, which in turn allowed for detailed analyses and interpretations of the data.

II. EXPERIMENTAL

X-ray Method

Measurements of the pressure dependence of the lattice parameter of ice VII were made by the energy dispersive powder diffraction method using a diamond anvil pressure cell[13]. The ruby fluorescence method was used to measure the pressure[14,15]. The pressure cell was mounted on a horizontal diffractometer equipped with a tungsten tube, an intrinsic germanium detector, and a 0.15 mm i.d. collimator made from telescoping sections of tungsten carbide tubing. An x, y, z micrometer stage was used for mounting and aligning the cell with respect to the x-ray beam and the diffractometer

axis. With proper alignment, patterns could be recorded with no trace of diffraction lines from the gasket. The sample was also centered on the axis of rotation so that it could be oscillated through ± 1.7° to reduce the effect of sample graininess, a severe problem because of the small sample volume (2×10^{-3} mm^3).

In addition to the 0.2° receiving slit, a 0.15 mm wide slit on the detector arm, 2.5 cm from the diffractometer axis, was used to exclude from the detector the radiation scattered along the path of the primary beam through the diamonds. This slit reduced the background counts by about a factor of ten over much of the energy range and greatly improved the signal-to-noise ratio.

A diffraction angle of $2\theta = 14.00°$ was selected. Assuming that the usable range of the x-ray continuum extends from 10 keV (below which less than 2 percent of the incident flux is transmitted by the diamonds) to 50 keV, the range of possible d spacings extends from 5.1 Å down to 1.0 Å, equivalent to the range obtained with a 2θ scan from 17° to 99° with CuKα radiation.

Generally the lattice parameter at each pressure was based on the (110), (200), and (211) reflections. The precision of the lattice parameter measurement was about 0.25 percent while the accuracy was about 1 percent. A more significant error resulted from the uncertainty of the pressure in the highest ranges arising from the nonhydrostatic character of ice VII. For example, the pressure measured by the ruby fluorescence method in a sample approximately 0.2 mm in diameter by 0.1 mm thick ranged from 23.7 GPa to 26.2 GPa. This range corresponds to 0.6 percent uncertainty in a and 0.8 percent uncertainty in $\Delta\bar{\nu}$. To circumvent this difficulty, the average pressure measured by ruby chips situated throughout the sample was employed.

Raman Method

Raman spectra of ice VII were obtained using the diamond anvil pressure cell and the ruby fluorescence method for pressure measurement. The spectra were obtained using two different double monochromators. For pressures to 15 GPa a standard Instruments S.A.* HG-2S instrument was employed, and for pressures from 15 to 30 GPa an HG-2S instrument equipped with red-sensitive holographic gratings was used. Detection was accomplished with cooled and uncooled Hamamatsu R928 (S-20) PM tubes, a Fluke 412B HV supply, a Keithley 414S picoammeter, an Esterline-Angus L1101S high-speed recorder, and at the highest pressures with a Nicolet multichannel analyzer. Slit-widths corresponding to 16 cm^{-1} were used in all cases, with scanning rates of 50 $cm^{-1}min^{-1}$. Excitation was accomplished with 514.5 and 488.0 nm excitation from Spectra Physics model 165 argon ion lasers. At pressures from 15 to 30 GPa, an interference filter was employed with 488.0 nm excitation.

The diamond anvil cell was used in two orientations. To pressures of 15 GPa, scattering at an acute angle was employed with collection in the forward direction[16]. At pressures from 15 to 30 GPa the acute angle scattering was also used but collection was accomplished in the backward direction. Pressures were measured simultaneously with Raman spectra by making comparisons between the fluorescence from the ruby in the cell, and from an external ruby in each run. Light scattered from an unfocussed laser beam at a power level of 100 mW was used in pressure measurements and care was taken not to focus on the ruby chips. In contrast a sharp focus was used in the ice to reduce the scattering from the diamonds during Raman measurements. No

*Certain commercial equipment, instruments, or materials are identified in this paper in order to adequately specify the experimental procedure. Such identification does not imply recommendation or endorsement by the National Bureau of Standards, nor does it imply that the materials or equipment identified are necessarily the best available for the purpose.

marked broadening and loss of detail in the two-phonon diamond band was observed in this work to 30 GPa.

For pressures up to 20 GPa, the precision of the Raman measurements was about 2 cm^{-1} while the accuracy was 5 cm^{-1}. Above 20 GPa, the accuracy was 10 cm^{-1}.

III. EXPERIMENTAL RESULTS

X-ray Data

The lattice parameters obtained for ice VII to 36 GPa are tabulated in Table I, and shown versus pressure in Fig. 1. From Fig. 1 it is apparent that the lattice parameter, a, (in Å) decreases at a decreasing rate with pressure rise. Various polynomials giving pressure P as a function of lattice parameter were fit to these data. Of these, a cubic fit using a digital computer with 72-bit words reproduced the data within 4 percent. The equation with pressure in GPa and lattice parameter in angstroms was as follows:

$$P = 7.8166 \times 10^3 - 6.8985 \times 10^3 (a) + 2.0368 \times 10^3 (a)^2 - 2.0114 \times 10^2 (a)^3. \quad (1a)$$

(The coefficients are given to five figures to represent the cubic equation accurately. These numbers should not be considered independently as significant figures.) The least squares fit is shown by the solid line through the data, Fig. 1.

Volumes determined from the present measurements differ by about 2.3 percent from Bridgman's early work[17]. There is good agreement with the results of Olinger and Halleck[18], when their revised pressure calibration is used[19]. An absolute comparison with the results reported by Holzapfel and Drickamer[20] could not be made because their absolute volume measurements were not given, but a relative comparison of V/V_o shows good agreement out to about 12.5 GPa.

The divergence observed at higher pressures can be attributed largely to the different pressure calibrations used which differ by about 2.6 percent at the higher pressures.

Raman Data

Raman OH-stretching peak frequencies obtained for ice VII to 30 GPa are tabulated in Table II, and plotted in Fig. 2. The peak frequency, $\Delta\bar{\nu}$, (in cm^{-1}) decreases at a decreasing rate with pressure rise. This decrease is similar to that observed for the x-ray data.

The Raman data were again treated by least squares polynomials. The fit of a cubic equation which reproduced the data within 3.8 percent with P as a function of $\Delta\bar{\nu}$, was as follows:

$$P = 6.7950 \times 10^{3} - 6.2337\,(\Delta\bar{\nu}) + 1.9164 \times 10^{-3}\,(\Delta\bar{\nu})^{2} - 1.9732 \times 10^{-7}\,(\Delta\bar{\nu})^{3}. \quad (1b)$$

(Again P is in GPa, $\Delta\bar{\nu}$ is in cm^{-1}, and the five digits do not independently represent significant figures.) The least squares fit is shown by the solid line, Fig. 2.

Raman spectra typical of those obtained in this work in the OH-stretching region are shown in Fig. 3 for pressures of 3.2 GPa and 15.5 GPa. In addition to the obvious decrease in the frequency of the Raman OH-stretching peak position, the shoulders, evident at 3.2 GPa between about 3350 cm^{-1} and 3600 cm^{-1}, also show frequency decreases with pressure rise. However, the shoulder intensities wane relative to the peak, making detection very difficult above about 10 to 15 GPa. When the OH-stretching peak is distinct from the shoulders, e.g., at 15.5 GPa, Fig. 3, the half-width (full width at half-height) of the peak corrected for slit width may be estimated, viz., 85 ± 15 cm^{-1}.

Correlation of Raman and X-ray Results

Method A-Linear Fit

The x-ray equation giving P as a function of a and the Raman equation giving P as a function of $\Delta\bar{\nu}$ were solved using $r_{00} = a\sqrt{3}/2$ to yield values of $\Delta\bar{\nu}$ versus r_{00} for uniformly selected values of r_{00} in the observed pressure range. To examine the functional dependence of $\Delta\bar{\nu}$ on r_{00}, polynomials in r_{00} were fit to the derived set of points. A first degree polynomial, $\Delta\bar{\nu} = -5.0725 \times 10^2 + 1.3135 \times 10^3\ r_{00}$, reproduced the data points to 0.2 percent. The slope of this linear relation, 1313.5 $cm^{-1}\text{Å}^{-1}$, is not too far from the value 1520 $cm^{-1}\text{Å}^{1}$ reported for ice I_h at 255 °K on the basis of Raman data[21]. In Fig. 4, the derived data points and the straight line fit (curve A) are shown. The gross trend of the data is clearly represented by the straight line in the observed range. However, extrapolation of the linear fit to small r_{00} values, e.g., to 2.4 Å or less, presents a serious difficulty. Such a linear extrapolation to r_{00} values below the value corresponding to a symmetric hydrogen bond, O-H-O, is thought to be equivalent to the physically erroneous situation in which the OH stretching force constant <u>decreases</u> as the OH bond <u>strengthens</u> by virtue of bond shortening. Hence, a cubic fit was tried, because the cubic extrapolation avoids a grossly false physical situation.

Method B--Cubic Fit

Data points for r_{00} values above about 2.7 Å were observed to deviate systematically from a straight line. This region involves the highest accuracy of the Raman and x-ray data, as well as pressure measurements, and it refers to a region of complete hydrostaticity. No method of data presentation, including plots of raw data, has thus far removed this curvature. To further test the validity of this nonlinearity, the deviation from a straight

line, compared to the uncertainty in $\Delta\bar{\nu}$ viewed as a function of r_{00}, was examined. An estimate of the uncertainty at the 95 percent confidence limit yields uncertainties of 0.056 percent for $0 < P < 10$ GPa; 0.98 percent for $10 < P < 17.5$ GPa; and 0.20 percent for $17.5 \text{ GPa} < P < 30$ GPa. On this basis, the straight line is an adequate representation of the details only for the highest pressure range, i.e., the smallest values of r_{00}. The largest excursion from a straight line occurs in the lowest pressure range at about $r_{00} = 2.785\text{Å}$ with a deviation of about 0.24 percent which is greater than the inherent uncertainty by more than a factor of 4. Therefore, for detailed accuracy, a higher order polynomial should be considered.

A quadratic equation reproduces the data points only to 0.15 percent, which is still not adequate. It also gives rise to a maximum at <u>low pressure</u>, and hence cannot also yield a minimum at high pressure. Therefore, its high pressure extrapolation involves the same problem mentioned previously with regard to the linear extrapolation. A cubic equation, however, successfully describes the data to 0.03 percent which is compatible with the uncertainty of $\Delta\bar{\nu}$ as shown by curve B in Fig. 4. The cubic equation is

$$\Delta\bar{\nu} = 7.8053 \times 10^4 - 8.6353 \times 10^4 \, r_{00} + 3.2573 \times 10^4 \, r_{00}^2 - 4.0297 \times 10^3 \, r_{00}^3.$$

The cubic fit also has the advantage that it yields a realistic high pressure extrapolation. At very high pressures a symmetric hydrogen bond, O-H-O, is expected to occur, and this would produce a minimum in the $\Delta\bar{\nu}$ vs r_{00} curve. The cubic equation thus allows an estimate of the symmetric hydrogen bond length to be made by finding the minimum which occurs in the extrapolation to smaller r_{00}. The cubic equation yields $r_{00}(\text{min}) = 2.35 \pm 0.06\text{Å}$, using a very conservative high pressure uncertainty in $\Delta\bar{\nu}$ of $\pm 20 \text{ cm}^{-1}$. Also using the pressure relation, P vs a, a corresponding value for P and its uncertainty can be determined. $P[r_{00}(\text{min})] = 75 \pm 20$ GPa.

This range of pressure agrees with a previous estimate of 35 to 80 GPa[11] and the r_{OO}(min) value agrees with a value of 2.4 Å presented subsequently.

Mode Grüneisen Parameter

The mode Grüneisen parameter is a nonthermodynamic quantity that can be determined from the volume dependence of a given vibrational (Raman or infrared) frequency. The definition for the ith Raman mode $\Delta\bar{\nu}_i$ is as follows:

$$\gamma_i = - \frac{\partial \ell n \Delta\bar{\nu}_i}{\partial \ell n v}, \tag{2}$$

where v is the cell volume. γ_i may be either positive or negative, but the total thermodynamic quantity, γ, where

$$\gamma = \sum_i \gamma_i \ , \tag{3}$$

is positive for most systems as seen from,

$$\gamma = v(\partial p/\partial T)_v/C_v = v(\partial S/\partial V)_T/C_v. \tag{4}$$

Values of γ_{OH} were calculated for the range of r_{OO} values from 2.35 to 3.035 Å, using both the method A and method B fits for $\Delta\bar{\nu}$ versus r_{OO}. The results are shown in Fig. 5.

γ_{OH} Values from Method A Fit

A plot of ln $\Delta\bar{\nu}$ vs ln a was found to be roughly linear, and to have a positive slope. Hence, $\gamma_{OH} \tilde{\sim}$ constant, from Eq. (2). To determine γ_{OH} as a function of r_{OO}, the linear fit, method A, Fig. 4, was employed. This procedure yielded the result labeled A in Fig. 5. The γ_{OH} from method A is roughly constant, but it shows a slight nearly-linear decrease with decreasing r_{OO}. In the region of data between 2.5 and 2.9 Å, the average value of γ_{OH}

is -0.39. This is close to the γ_{OH} of -0.36 reported for the OH stretching mode of ice I_h[23]. However, the decreasing trend of γ_{OH} with decreasing r_{OO} leads to the same unrealistic physical situation mentioned previously for the linear extrapolation of Fig. 4.

γ_{OH} Values from Method B Fit

In Fig. 5, γ_{OH} values determined from the method B cubic fit of the Fig. 4 data are shown, labeled B. Here a quadratic dependence between γ_{OH} and r_{OO} is evident which yields a minimum near 2.7 Å. The average value of γ_{OH} in the region of data between 2.5 and 2.9 Å is -0.36 in agreement with the value of -0.36 reported for ice I_h[23]. The extrapolation of γ_{OH} to large, 3.035 Å, and small, 2.35 Å, values of r_{OO} using method B is shown by the dashed line in Fig. 5 (also for method A). The high pressure extrapolation suggests that γ_{OH} may become positive at pressures where symmetric O-H-O units occur. The reasons for this are described subsequently.

The negative values of γ_{OH} obtained either by method A or B imply from Eq. (4) that other vibrational modes must have positive γ_i values. Ice I_h, for example, has a γ_i value of 1.86 for the intermolecular O-O stretching mode[23], whereas the intramolecular OH-stretching vibration has a γ_{OH} of -0.36. A similar situation is expected to occur for ice VII at low pressures.

IV. INTERPRETATION

Relationship Between r_{OH} and r_{OO}.

An approximate treatment leading to an inverse square relationship between r_{OH} and $\Delta\bar{\nu}$ follows. This approach treats a hydrogen bond in ice VII as a weakly coupled oscillator system, and refers specifically to the weak-coupling region $2.54 < r_{OO} < 2.90$ Å. The treatment does not apply to values of $r_{OO} \ll 2.54$, where the coupling between O-H and H····O of the O-H····O bonds probably becomes extremely strong.

Consider a hydrogen bond, O-H····O, as a weakly coupled oscillator system having a force constant k_1 for the OH bond and a force constant k_2 for the weak H····O liaison. The system is pictured schematically in Fig. 6. In the O-H····O linkage the OH distance is r_{OH}, the H····O distance, r_{HO}, and $r_{OO} = r_{OH} + r_{HO}$. If the magnitude of the proton displacement from its equilibrium position is d, the absolute magnitude of the harmonic restoring force opposing this displacement is given by,

$$F = k_1 d + k_2 d, \tag{5}$$

or by

$$F = \frac{\mathcal{K}_1 d}{r_{OH}} + \frac{\mathcal{K}_2 d}{r_{HO}} , \tag{6}$$

where $\mathcal{K}_1$ and $\mathcal{K}_2$ are the elastic moduli[24] corresponding to the OH and H····O bonds, respectively. For convenience, let $F' = F/d$, whence,

$$F' = \frac{\mathcal{K}_1}{r_{OH}} + \frac{\mathcal{K}_2}{r_{HO}} . \tag{7}$$

Next, it is assumed that $\mathcal{K}_1 >> \mathcal{K}_2$, i.e., weak coupling. Further it is assumed that $\mathcal{K}_1$ is constant, i.e., $\neq f(r_{OO})$. (This assumption may not be exact, but it has the effect of forcing all of the change in $\mathcal{K}_1$ to occur via a change in r_{OH}. Also, the increase in r_{OH} for $2.54 < r_{OO} < 2.90$ Å is estimated to be only about 9 percent.) Equation 6 is thus reduced to

$$F' \approx \frac{\mathcal{K}_1}{r_{OH}} , \qquad \text{and} \tag{8}$$

differentiation with respect to r_{OO} gives,

$$\frac{dF'}{dr_{OO}} = - \frac{\kappa_1}{r^2_{OH}} \frac{dr_{OH}}{dr_{OO}} \quad . \tag{9}$$

Further for a harmonic oscillator, $F' = c\omega^2$, where c is a constant, and ω is the vibrational frequency in cm^{-1}. Differentiation gives $dF' = 2c\omega d\omega$, and substitution in Eq. (8) yields,

$$\frac{2c\omega d\omega}{dr_{OO}} \simeq - \frac{\kappa_1}{r^2_{OH}} \frac{dr_{OH}}{dr_{OO}} \quad . \tag{10}$$

Taking $d\omega/dr_{OO}$ approximately constant = β, as seen from A in Fig. 4, and assuming also that $dr_{OH}/dr_{OO} = -\alpha$ = constant, then

$$\omega \simeq \frac{\alpha\kappa_1}{2c\beta} \frac{1}{r^2_{OH}} \quad , \tag{11}$$

or,

$$\Delta\bar{\nu} \simeq A/r^2_{OH}, \tag{12}$$

where $\omega = \Delta\bar{\nu}$, and $A = \alpha\kappa_1/2c\beta$.

Equation (12) has been tested in the following manner assuming that the relationship between r_{OO} and r_{OH} is the same whether deduced for (A) systems of differing chemical elements at one pressure, or (B) a given system in which changes in bond distances are induced by changes in pressure. In recent work, a plot of r_{OH} versus r_{OO} for various hydrogen-bonded systems, at one atmosphere of pressure and having O-H-O angles greater than 160°, was given[25] using carefully selected neutron and x-ray data. Data from that work have been reproduced in Fig. 7. In the region of interest, $2.54 < r_{OO} < 2.90$ Å, the approximation of dr_{OH}/dr_{OO} = contant = $-\alpha$ is satisfied with $\alpha = 0.24$. For each r_{OO} in Fig. 7, a value of $\Delta\bar{\nu}$ was determined

from the cubic equation used in Fig. 4 which was determined for one system (H_2O, ice VII) under pressure. This gave a new set of values, $\Delta\bar{\nu}$ versus r_{OH}, to which Eq. (12) was fit. The value A = 2943 cm^{-1} $Å^2$ was obtained, and this produced the solid curve shown in Fig. 7. Additionally, it can also be seen from Fig. 7, as obtained from Ref. (25), that the symmetric O-H-O unit, i.e., $r_{OO} = 2r_{OH}$ occurs at 2.4 Å for other materials. This compares very favorably with our own estimate of 2.35 ± 0.06 Å.

Equation (12) and its derivation, albeit approximate, lead to implications of relevance to all the results of this work.

When pressure is applied to ice VII, a, and thus r_{OO}, decrease at a decreasing rate, Fig. 1. Pressures in excess of 36 GPa would only be expected to produce a further decrease in r_{OO}, with the rate of decrease continuing to decline. No minimum in the curve of r_{OO} versus pressure would be expected.

The plot of $\Delta\bar{\nu}$ versus pressure, Fig. 2, has a curvature similar to that of Fig. 1. In contrast to the x-ray data, however, a minimum in $\Delta\bar{\nu}$ would be expected to occur at some very high pressure, e.g., as shown by curve B in Fig. 4. Further, Fig. 2 is thought to indicate that the OH-stretching force constant decreases with pressure rise because the OH bond is lengthening. However, a pressure, P_s, will eventually be obtained at which $r_{OH} = r_{OO}/2$. Above this pressure, i.e., when $P > P_s$, the OH distance may decrease at the same rate as the O-O distance decreases (provided that r_{OH} continues to equal $r_{OO}/2$). If the OH bond distance decreases, the OH force constant will increase, and $\Delta\bar{\nu}$ will <u>increase</u>. Hence, a minimum in $\Delta\bar{\nu}$ versus P, or in $\Delta\bar{\nu}$ versus r_{OO}, is expected, Fig. 4 curve B.

Associated with the occurrence of a minimum in $\Delta\bar{\nu}$ vs r_{OO} would be a change of sign for the mode Grüneison parameter γ_{OH}. This would occur because for $P > P_S$, $\Delta\bar{\nu}$ would increase with increasing pressure while the volume

would continue to decrease. Hence, by Eq. (2), γ_{OH} would be positive for $P > P_S$. At room pressure, γ_{OH} is negative and decreases with an increase of pressure. Consequently, the hypothesis of a symmetric hydrogen bond at high pressure and the values of γ_{OH} at low pressure imply that γ_{OH} vs r_{OO} has a minimum negative value and rises to zero at the high pressure symmetric bond length. The values of γ_{OH} computed by method B and their smooth curve extrapolation, which are shown in Fig. 5, exhibit this behavior.

The minimum of γ_{OH} vs r_{OO} may possibly be understood in terms of the approaching dominance of the repulsive part of the potential. It is known, for example, that γ generally increases with density when the repulsive part of the potential behaves like that for hard spheres[26]. This situation may be analogous to that of symmetric ice VII. This ice may no longer contain discrete H_2O molecules and may be ionic and proton ordered as the result of symmetric O-H-O units. This situation is possible because the r_{OH} distance increases with pressure rise, and thus the s-p orbital overlap between H and O may decrease, leading to higher ionic OH character compared to isolated H_2O molecules. Also, extremely strong O-O repulsive forces, resembling those between hard spheres at high density, would be present.

Finally, other features of the present results are of some interest. Figure 4 shows a minimum in $\Delta\bar{\nu}$ at 2712 cm^{-1} for r_{OO} = 2.35 Å, and a maximum in $\Delta\bar{\nu}$ of 3355 cm^{-1} at r_{OO} = 3.04 Å. The pressure corresponding to the minimum $\Delta\bar{\nu}$ is estimated to be 75 ± 20 GPa. Extrapolation of the cubic relation to the maximum is not meaningful because the maximum occurs in a physically unobservable region[27]. In regard to this, the Raman data of Fig. 2 below 5 GPa were treated by a first degree polynomial with $\Delta\bar{\nu}$ as a function of P. For P = 0, which essentially corresponds to the maximum feature in Fig. 4, $\Delta\bar{\nu}$ = 3378 cm^{-1}. The value of 3378 cm^{-1} may refer to an upper limit, as opposed

to a maximum, of the vibrational frequency when the OH bond in the linear O-H···O linkage of ice VII has its smallest length. From Fig. 7 this would correspond to 0.94 Å, which in view of the scatter of the data is not much different from the gas phase value of 0.96 Å[25].

V. ACKNOWLEDGMENTS

This work was supported in part by a grant from the National Science Foundation, Chemical Thermodynamics Program, CHE77-09888, and by a contract, Laser-chemistry, from the Office of Naval Research. Helpful discussions with F. H. Stillinger, E. Whalley, B. Kamb, and W. B. Holzapfel are gratefully acknowledged.

REFERENCES

1. P. W. Bridgman, J. Chem. Phys. 5, 946 (1937).
2. C. W. F. T. Pistorius, E. Rapoport, and J. B. Clark, J. Chem. Phys. 48, 5509 (1968).
3. B. Kamb and B. L. Davis, Proc. Nat. Acad. Sci. U.S. 52, 1433 (1964).
4. C. E. Weir, S. Block, and G. J. Piermarini, J. Res. Nat. Bur. Stds. 69C, 275 (1965).
5. G. P. Johari, A. Lavergne, and E. Whalley, J. Chem. Phys. 61, 4292 (1974).
6. B. Kamb, quoted in "Ice Physics", P. V. Hobbs, Clarendon, Oxford, 1974.
7. B. Kamb and A. Prakash, quoted in "Ice Physics", P. V. Hobbs, Clarendon, Oxford 1974.
8. C. W. F. T. Pistorius, Prog. in Solid State Chemistry, 11, 1 (1976).
9. G. J. Piermarini and S. Block, Rev. Sci. Instrum. 46, 978 (1975).
10. S. Block and G. J. Piermarini, unpublished.
11. W. B. Holzapfel, J. Chem. Phys. 56, 712 (1972).
12. M. Abebe and G. E. Walrafen, J. Chem. Phys. 71, 4167 (1979).
13. F. A. Mauer, S. Block, and G. J. Piermarini, Paper G3, American Crystallographic Association, Program and Abstracts of Summer Meeting, Boston University, Boston, MA, August 12-17, 1979.
14. J. D. Barnett, S. Block, and G. J. Piermarini, Rev. Sci. Instrum. 44, 1 (1973).
15. G. J. Piermarini, S. Block, J. D. Barnett, and R. A. Forman, J. Appl. Phys. 46, 2774 (1975).
16. C. H. Whitfield, E. M. Brody, and W. A. Bassett, Rev. Sci. Instrum. 47, 942 (1976).
17. P. W. Bridgman, Proc. Amer. Acad. Arts Sci. 74, 399 (1942).
18. B. Olinger and P. M. Halleck, J. Chem. Phys. 62, 94 (1975).
19. B. Olinger and H. Cady, Proceedings Sixth Symposium (International) on Detonation, Corondado, CA, August 1976, p. 700.
20. W. B. Holzapfel and H. G. Drickamer, J. Chem. Phys. 48, 4798 (1968).

21. T. C. Sivakumar, H. A. M. Chew, and G. P. Johari, Nature 275, 524 (1978).

22. To be published.

23. G. P. Johari and T. C. Sivakumar, J. Chem. Phys. 69, 5557 (1978).

24. Classically, $\gamma_i = A_i Y_i$ where A_i is the area and Y_i is Young's modulus, but in the present work, A_{OH} relates roughly to the electron density in the O-H bond, and Y_{OH} relates roughly to the OH bond strength.

25. J. C. Speakman, MTP International Review of Science, Physical Chemistry Series One, Vol. II, (Chemical Crystallography) J. M. Robertson, ed, Butterworths, University Park Press, Baltimore, MD, pp. 1-31, 1972.

26. B. J. Alder, Physics Experiments with Strong Pressure Pulses, Chap. 13, in Solids Under Pressure, W. Paul and D. M. Warschauer, eds., McGraw-Hill, NY, (1963).

27. Ice VII does not usually exist at this pressure except when quenched at low temperatures. The maximum in Fig. 4 refers to a metastable condition thus far unreported at room temperature.

FIGURE CAPTIONS

1. X-ray lattice parameter, a, in Å, versus pressure in GPa for ice VII at room temperature.
2. Raman OH-stretching peak frequencies $\Delta\bar{\nu}$, in cm^{-1}, versus pressure in GPa for ice VII at room temperature.
3. Raman spectra in the OH-stretching region for ice VII at 3.2 and 15.5 GPa.
4. Raman versus x-ray correlations, $\Delta\bar{\nu}_{OH}$ versus r_{OO}, for ice VII. Points, computed from least squares equations for P as a function of a and P as a function of $\Delta\bar{\nu}_{OH}$, see text. Curve A refers to a linear and curve B to a cubic least squares fit to the computed points.
5. Mode Grüneisen parameter, γ_{OH}, computed from method A (linear) and method B (cubic) least squares fits of $\Delta\bar{\nu}$ versus r_{OO}, see Fig. 4 and text. Points shown delineate region of x-ray and Raman data. Dashed lines refer to extrapolations according to method A or method B.
6. Weakly coupled oscillator model for the hydrogen bonds in ice VII. The O-H force constant is k_1, and k_2 is the force constant for H····O. The figure defines relevant distances with d being the proton displacement from its equilibrium position.
7. Plot of r_{OH} versus r_{OO} both in Å for hydrogen-bonded systems. Points from Speakman, ref. 25. Solid line computed from x-ray and Raman data for ice VII.

TABLE CAPTIONS

I. X-ray lattice parameter data for ice VII to 36 GPa.

II. Raman OH-stretching peak frequency data for ice VII to 30 GPa.

Table I

p,GPa	a,Å
2.30	3.368
2.30	3.365
2.85	3.337
4.76	3.268
5.45	3.256
6.20	3.231
8.85	3.166
10.07	3.154
11.64	3.109
11.65	3.106
12.47	3.110
14.04	3.078
15.05	3.074
15.58	3.048
15.58	3.045
17.70	3.042
17.95	3.035
19.57	3.029
20.13	3.008
20.32	3.013
23.40	3.011
24.30	2.961
24.57	2.966
24.58	2.968
26.50	2.974
26.50	2.970
29.65	2.940
30.00	2.923
36.00	2.896

Table II

p,GPa	$\Delta\bar{\nu}$,cm^{-1}	p,GPa	$\Delta\bar{\nu}$,cm^{-1}
2.04	3308.	8.10	3124.
2.06	3310.	8.24	3102.
2.06	3304.	8.30	3122.
2.08	3306.	8.57	3110.
2.12	3298.	8.63	3102.
2.18	3305.	8.76	3100.
2.18	3310.	9.50	3074.
2.18	3299.	9.60	3082.
2.26	3308.	9.60	3092.
2.38	3308.	9.90	3075.
2.39	3305.	10.70	3050.
2.49	3286.	10.83	3045.
2.56	3288.	10.89	3040.
2.61	3301.	10.90	3044.
2.62	3291.	10.90	3050.
2.62	3288.	11.00	3062.
2.69	3288.	11.49	3028.
3.02	3273.	12.50	3025.
3.19	3263.	12.67	3027.
4.32	3235.	13.41	3009.
4.44	3230.	13.68	3013.
4.78	3216.	13.96	3003.
5.18	3213.	14.01	3001.
5.68	3185.	14.21	2997.
5.84	3180.	14.38	2990.
6.10	3170.	14.63	2994.
6.37	3163.	14.75	2974.
6.38	3155.	14.99	2982.
6.50	3166.	15.29	2975.
6.80	3160.	15.50	2982.
7.26	3147.	19.30	2931.
7.60	3150.	22.80	2893.
7.70	3143.	26.40	2848.
7.82	3109.	30.00	2831.

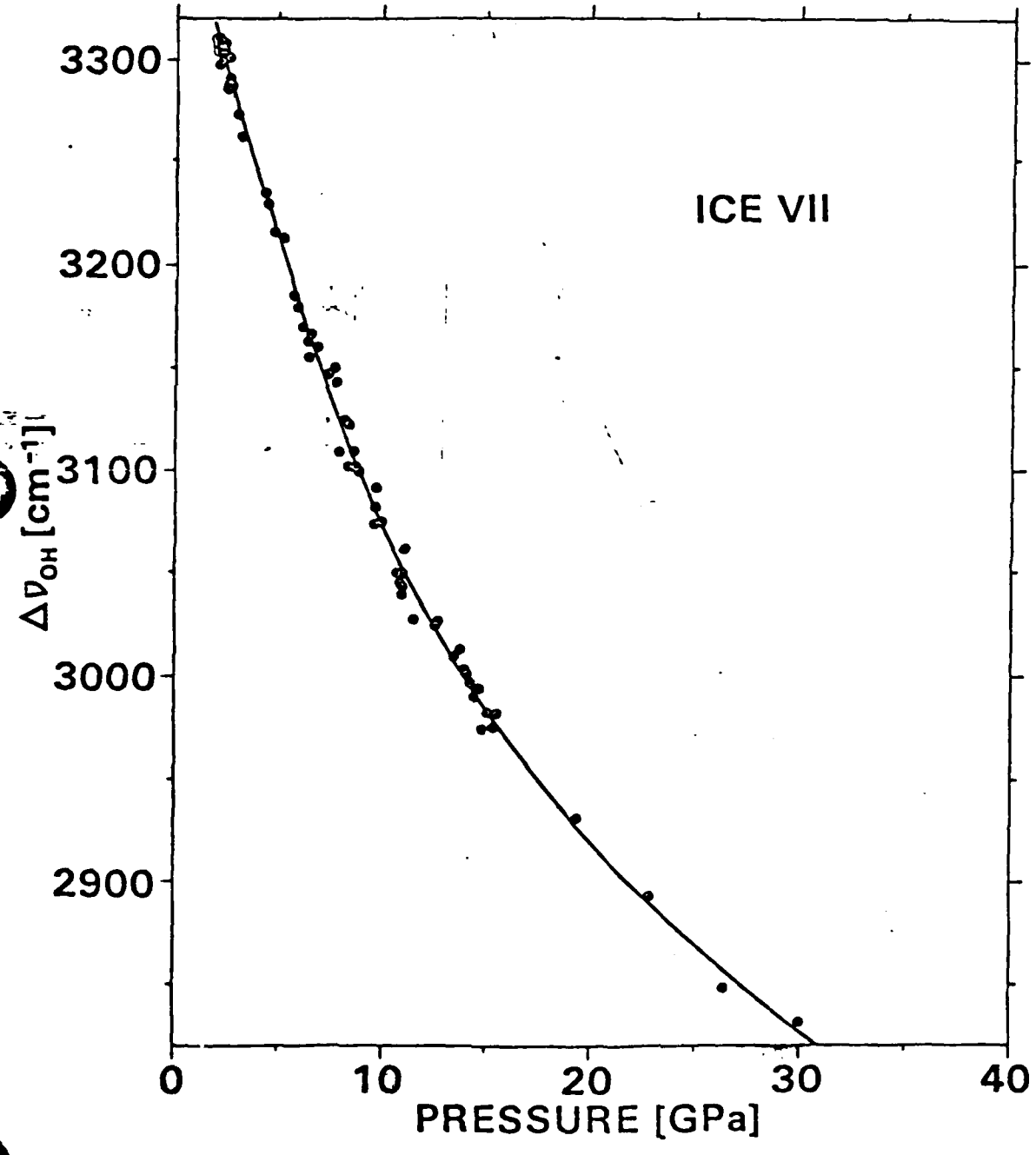
ICE VII
3300
3200
3100
3000
2900
$\Delta\nu_{OH}$ [cm^{-1}]
0
10
20
30
40
PRESSURE [GPa]

FIGURE 2

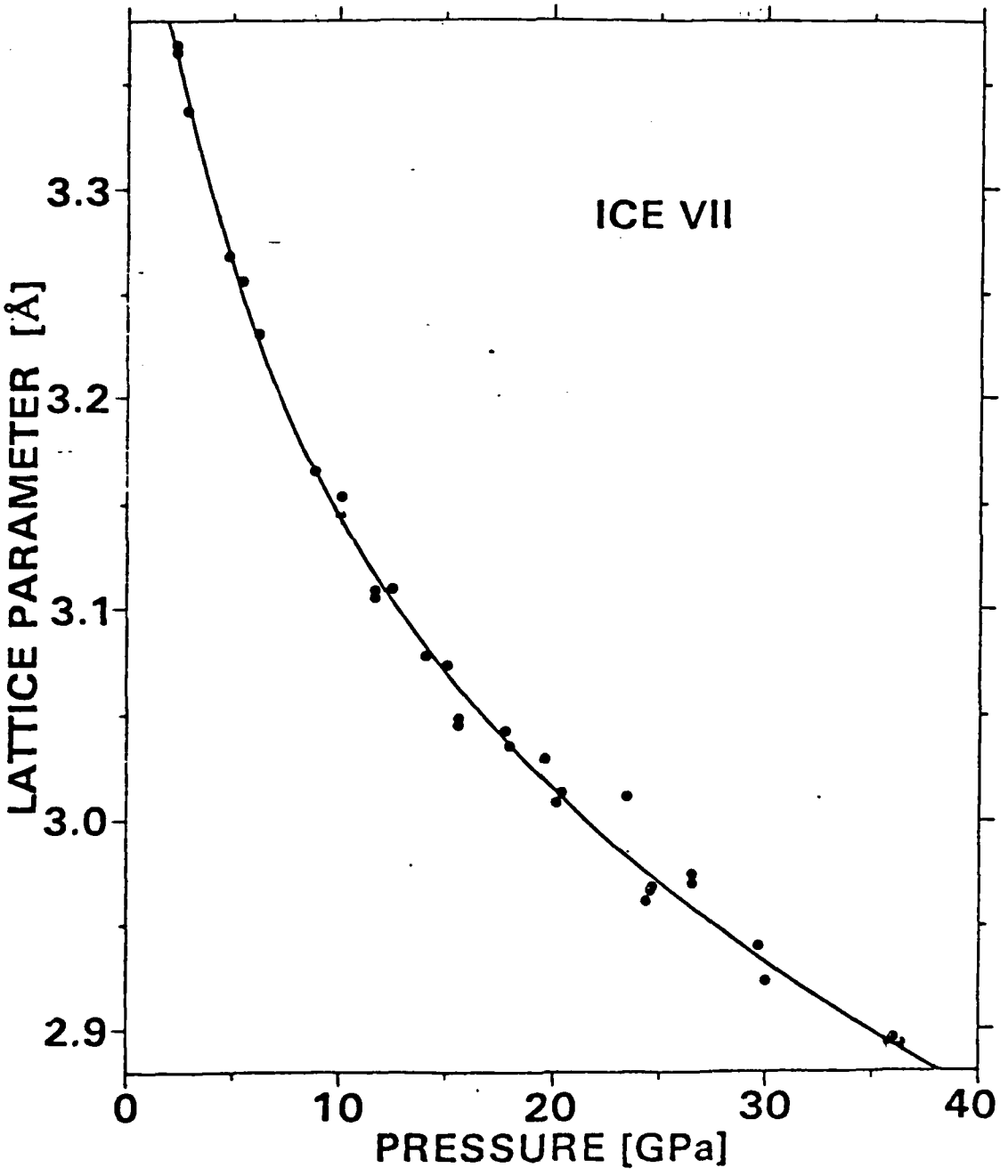
ICE VII
LATTICE PARAMETER [Å]
3.3
3.2
3.1
3.0
2.9
0
10
20
30
40
PRESSURE [GPa]

FIGURE 1

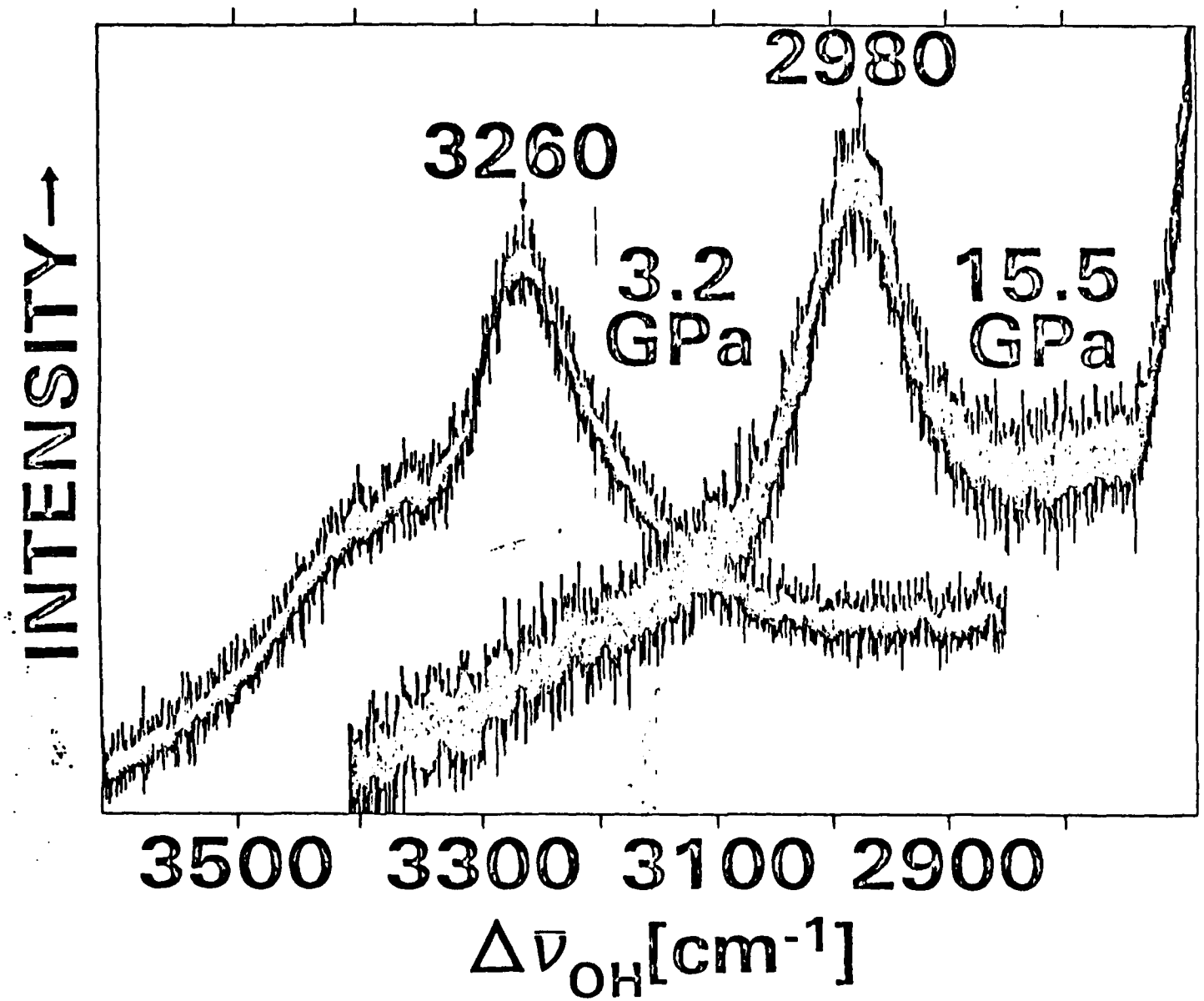
2980
3260
3.2
GPa
15.5
GPa
INTENSITY→
3500 3300 3100 2900
$\Delta\bar{\nu}_{OH}$[cm^{-1}]

FIGURE 3

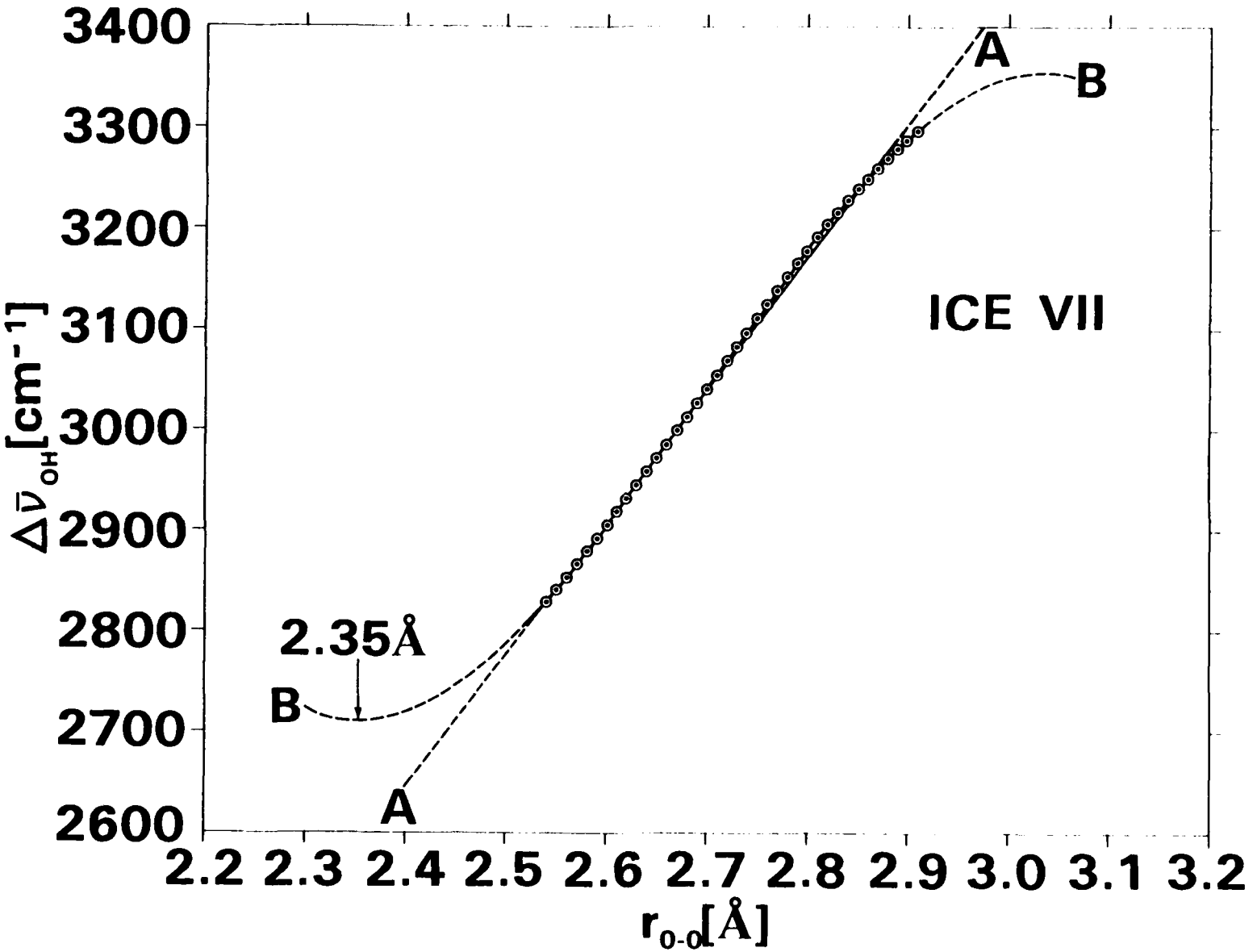
3400
3300
3200
3100
3000
2900
2800
2700
2600
$\Delta\bar{\nu}_{OH}$[cm^{-1}]
2.2 2.3 2.4 2.5 2.6 2.7 2.8 2.9 3.0 3.1 3.2
$r_{O\text{-}O}$[Å]
A
B
2.35Å
B
A
ICE VII

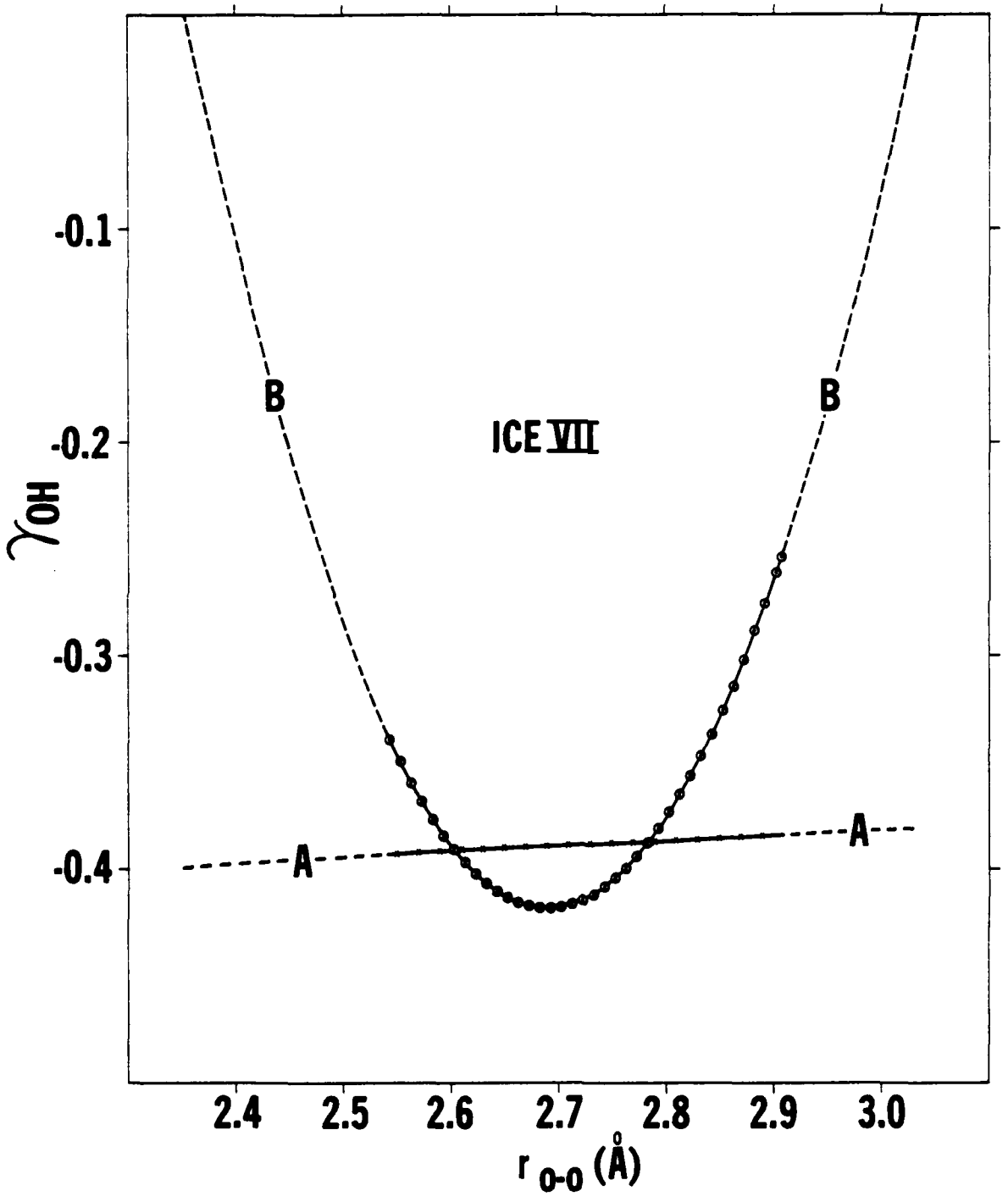
-0.1
-0.2
-0.3
-0.4
γ_{OH}
B
B
ICE VII
A
A
2.4
2.5
2.6
2.7
2.8
2.9
3.0
r_{O-O} (Å)

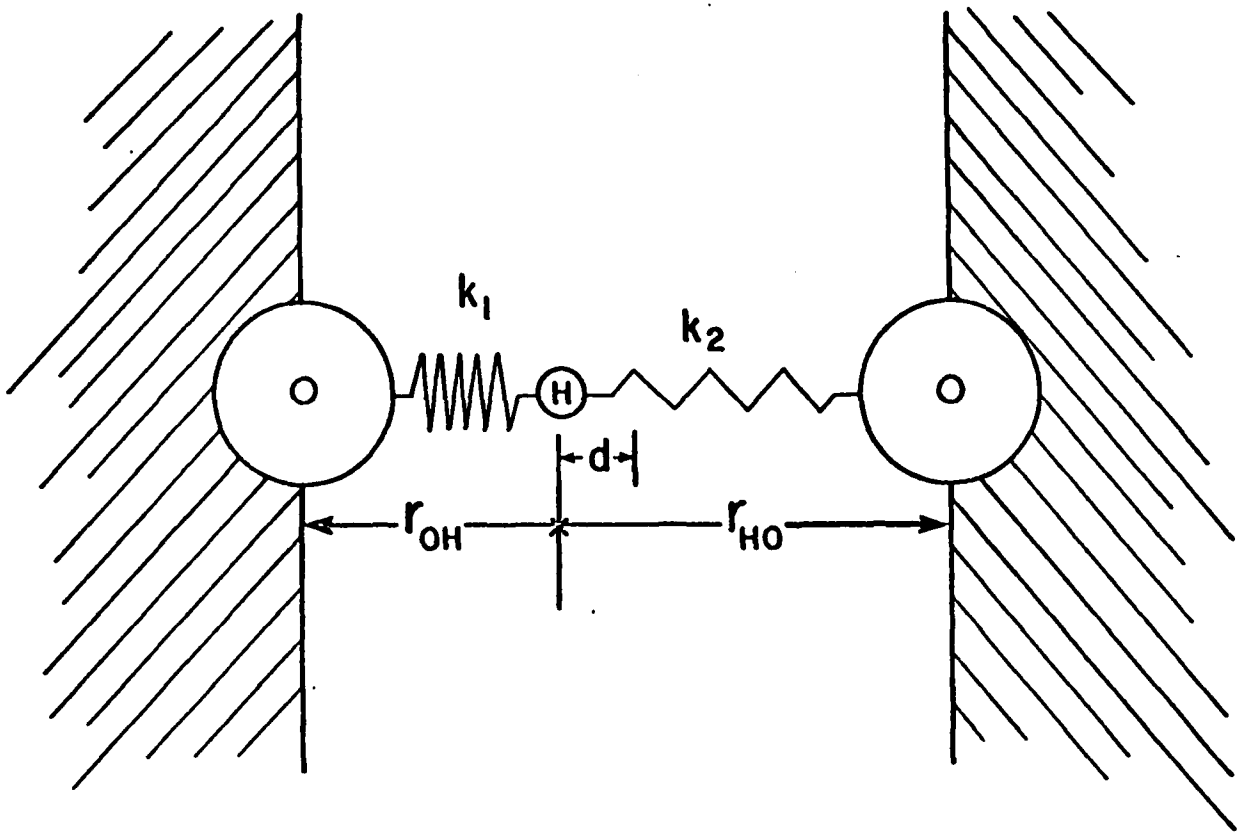
k1
k2
O
H
O
d
r_{OH}
r_{HO}

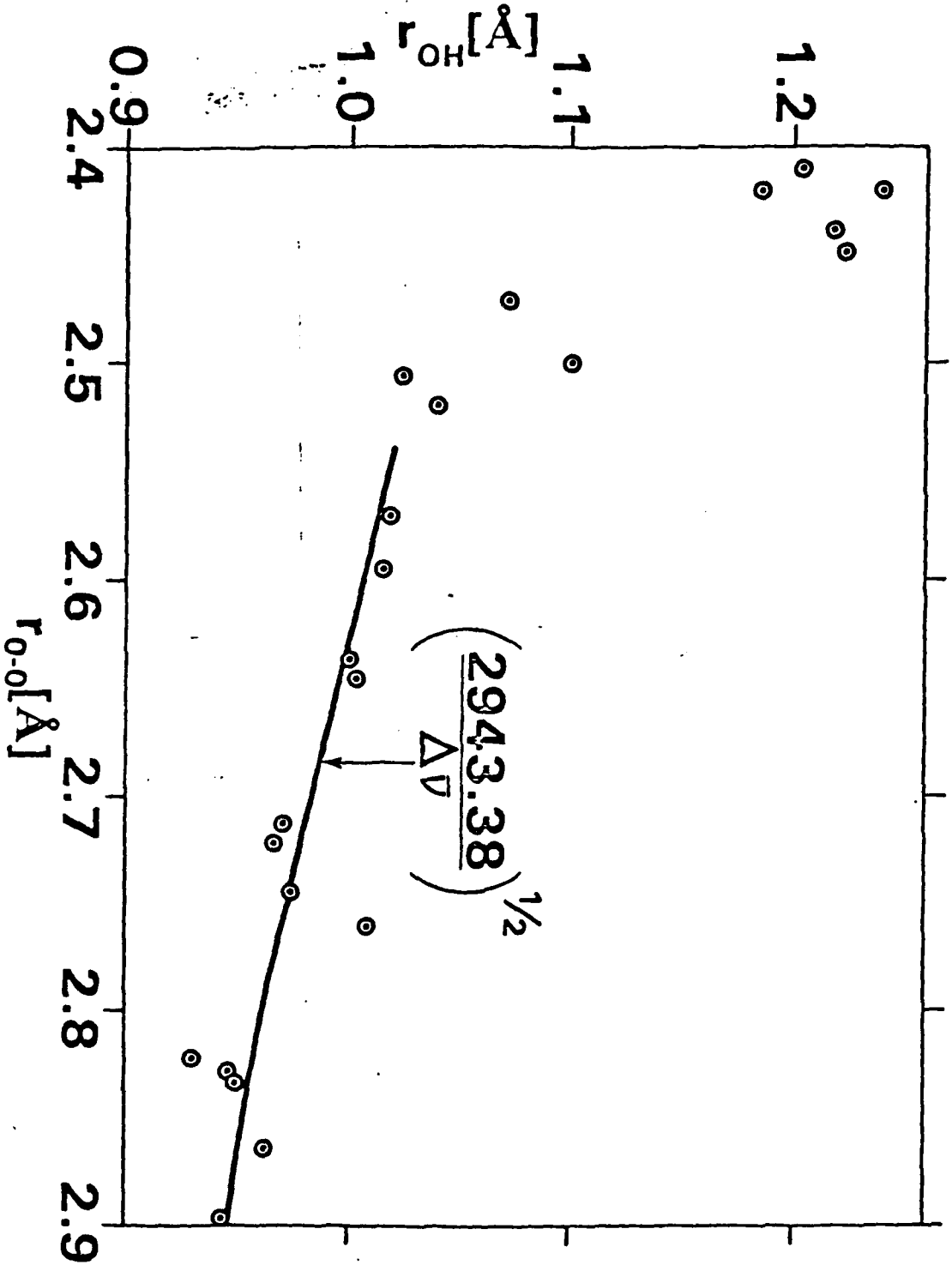
r_{OH}[Å]
0.9
1.0
1.1
1.2
$r_{O\text{-}O}$[Å]
2.4
2.5
2.6
2.7
2.8
2.9
$\left(\frac{2943.38}{\Delta\nu}\right)^{1/2}$

FIGURE 7

472:CAN:716:ddc
78u472-608

TECHNICAL REPORT DISTRIBUTION LIST, GEN

	No. Copies
Office of Naval Research Attn: Code 472 800 North Quincy Street Arlington, Virginia 22217	2
ONR Branch Office Attn: Dr. George Sandoz 536 S. Clark Street Chicago, Illinois 60605	1
ONR Area Office Attn: Scientific Dept. 715 Broadway New York, New York 10003	1
ONR Western Regional Office 1030 East Green Street Pasadena, California 91106	1
ONR Eastern/Central Regional Office Attn: Dr. L. H. Peebles Building 114, Section D 666 Summer Street Boston, Massachusetts 02210	1
Director, Naval Research Laboratory Attn: Code 6100 Washington, D.C. 20390	1
The Assistant Secretary of the Navy (RE&S) Department of the Navy Room 4E736, Pentagon Washington, D.C. 20350	1
Commander, Naval Air Systems Command Attn: Code 310C (H. Rosenwasser) Department of the Navy Washington, D.C. 20360	1
Defense Technical Information Center Building 5, Cameron Station Alexandria, Virginia 22314	12
Dr. Fred Saalfeld Chemistry Division, Code 6100 Naval Research Laboratory Washington, D.C 20375	1
U.S. Army Research Office Attn: CRD-AA-IP P.O. Box 1211 Research Triangle Park, N.C. 27709	1
Naval Ocean Systems Center Attn: Mr. Joe McCartney San Diego, California 92152	1
Naval Weapons Center Attn: Dr. A. B. Amster, Chemistry Division China Lake, California 93555	1
Naval Civil Engineering Laboratory Attn: Dr. R. W. Drisko Port Hueneme, California 93401	1
Department of Physics & Chemistry Naval Postgraduate School Monterey, California 93940	1
Dr. A. L. Slafkosky Scientific Advisor Commandant of the Marine Corps (Code RD-1) Washington, D.C. 20380	1
Office of Naval Research Attn: Dr. Richard S. Miller 800 N. Quincy Street Arlington, Virginia 22217	1
Naval Ship Research and Development Center Attn: Dr. G. Bosmajian, Applied Chemistry Division Annapolis, Maryland 21401	1
Naval Ocean Systems Center Attn: Dr. S. Yamamoto, Marine Sciences Division San Diego, California 91232	1
Mr. John Boyle Materials Branch Naval Ship Engineering Center Philadelphia, Pennsylvania 19112	1

TECHNICAL REPORT DISTRIBUTION LIST, 051A

	No. Copies
Dr. M.A. El-Sayed Department of Chemistry University of California, Los Angeles Los Angeles, California 90024	1
Dr. E. R. Bernstein Department of Chemistry Colorado State University Fort Collins, Colorado 80521	1
Dr. C. A. Heller Naval Weapons Center Code 6059 China Lake, California 93555	1
Dr. J. R. MacDonald Chemistry Division Naval Research Laboratory Code 6110 Washington, D.C. 20375	1
Dr. G. B. Schuster Chemistry Department University of Illinois Urbana, Illinois 61801	1
Dr. A. Adamson Department of Chemistry University of Southern California Los Angeles, California 90007	1
Dr. M. S. Wrighton Department of Chemistry Massachusetts Institute of Technology Cambridge, Massachusetts 02139	1
Dr. M. Rauhut Chemical Research Division American Cyanamid Company Bound Brook, New Jersey 08805	1
Dr. J. I. Zink Department of Chemistry University of California, Los Angeles Los Angeles, California 90024	1
Dr. D. Haarer IBM San Jose Research Center 5600 Cottle Road San Jose, California 95143	1
Dr. John Cooper Code 6130 Naval Research Laboratory Washington, D.C. 20375	1
Dr. William M. Jackson Department of Chemistry Howard University Washington, DC 20059	1
Dr. George E. Walraffen Department of Chemistry Howard University Washington, DC 20059	1

	No. Copies
Dr. Rudolph J. Marcus Office of Naval Research Scientific Liaison Group American Embassy APO San Francisco 96503	1
Mr. James Kelley DTNSRDC Code 2303 Annapolis, Maryland 21402	1

TECHNICAL REPORT DISTRIBUTION LIST, 051A

	No. Copies
Dr. M.A. El-Sayed Department of Chemistry University of California, Los Angeles Los Angeles, California 90024	1
Dr. E. R. Bernstein Department of Chemistry Colorado State University Fort Collins, Colorado 80521	1
Dr. C. A. Heller Naval Weapons Center Code 6059 China Lake, California 93555	1
Dr. J. R. MacDonald Chemistry Division Naval Research Laboratory Code 6110 Washington, D.C. 20375	1
Dr. G. B. Schuster Chemistry Department University of Illinois Urbana, Illinois 61801	1
Dr. A. Adamson Department of Chemistry University of Southern California Los Angeles, California 90007	1
Dr. M. S. Wrighton Department of Chemistry Massachusetts Institute of Technology Cambridge, Massachusetts 02139	1
Dr. M. Rauhut Chemical Research Division American Cyanamid Company Bound Brook, New Jersey 08805	1
Dr. J. I. Zink Department of Chemistry University of California, Los Angeles Los Angeles, California 90024	1
Dr. D. Haarer IBM San Jose Research Center 5600 Cottle Road San Jose, California 95143	1
Dr. John Cooper Code 6130 Naval Research Laboratory Washington, D.C. 20375	1
Dr. William M. Jackson Department of Chemistry Howard University Washington, DC 20059	1
Dr. George E. Walraffen Department of Chemistry Howard University Washington, DC 20059	1

	No. Copies
Dr. Rudolph J. Marcus Office of Naval Research Scientific Liaison Group American Embassy APO San Francisco 96503	1
Mr. James Kelley DTNSRDC Code 2803 Annapolis, Maryland 21402	1


ED
8